

Title	The structural and piezoresponse properties of c-axis-oriented Aurivillius phase Bi ₅ Ti ₃ FeO ₁₅ thin films deposited by atomic vapor deposition
Authors	Zhang, Panfeng F.;Deepak, Nitin;Keeney, Lynette;Pemble, Martyn E.;Whatmore, Roger W.
Publication date	2012-09-11
Original Citation	Zhang, P. F., Deepak, N., Keeney, L., Pemble, M. E. and Whatmore, R. W. (2012) 'The structural and piezoresponse properties of c-axis-oriented Aurivillius phase Bi ₅ Ti ₃ FeO ₁₅ thin films deposited by atomic vapor deposition'. Applied Physics Letters, 101, 112903. http://scitation.aip.org/content/aip/journal/apl/101/11/10.1063/1.4752007
Type of publication	Article (peer-reviewed)
Link to publisher's version	10.1063/1.4752007
Rights	© 2012 American Institute of Physics. This article may be downloaded for personal use only. Any other use requires prior permission of the author and AIP Publishing. The following article appeared in Appl. Phys. Lett. 101, 112903 (2012) and may be found at http://scitation.aip.org/content/aip/journal/apl/101/11/10.1063/1.4752007
Download date	2025-08-02 04:40:01
Item downloaded from	https://hdl.handle.net/10468/2933



UCC

University College Cork, Ireland
Coláiste na hOllscoile Corcaigh

The structural and piezoresponse properties of c-axis-oriented Aurivillius phase Bi₅Ti₃FeO₁₅ thin films deposited by atomic vapor deposition

P. F. Zhang, N. Deepak, L. Keeney, M. E. Pemble, and R. W. Whatmore

Citation: *Appl. Phys. Lett.* **101**, 112903 (2012); doi: 10.1063/1.4752007

View online: <http://dx.doi.org/10.1063/1.4752007>

View Table of Contents: <http://apl.aip.org/resource/1/APPLAB/v101/i11>

Published by the [American Institute of Physics](#).

Related Articles

How are the behaviors of piezoelectric inertial sliders interpreted?

Rev. Sci. Instrum. **83**, 093701 (2012)

Current-voltage characteristics and ON/OFF ratio in ferroelectric tunnel junctions

J. Appl. Phys. **112**, 054102 (2012)

Flexoelectricity in several thermoplastic and thermosetting polymers

Appl. Phys. Lett. **101**, 103905 (2012)

Piezoresponse force microscopy characterization of high aspect ratio ferroelectric nanostructures

J. Appl. Phys. **112**, 052012 (2012)

Direct determination of the effect of strain on domain morphology in ferroelectric superlattices with scanning probe microscopy

J. Appl. Phys. **112**, 052011 (2012)

Additional information on *Appl. Phys. Lett.*

Journal Homepage: <http://apl.aip.org/>

Journal Information: http://apl.aip.org/about/about_the_journal

Top downloads: http://apl.aip.org/features/most_downloaded

Information for Authors: <http://apl.aip.org/authors>

ADVERTISEMENT



HAVE YOU HEARD?

Employers hiring scientists
and engineers trust
physicstodayJOBS

<http://careers.physicstoday.org/post.cfm>



The structural and piezoresponse properties of *c*-axis-oriented Aurivillius phase $\text{Bi}_5\text{Ti}_3\text{FeO}_{15}$ thin films deposited by atomic vapor deposition

P. F. Zhang,^{a)} N. Deepak, L. Keeney, M. E. Pemble, and R. W. Whatmore
Tyndall National Institute, University College Cork, Lee Maltings, Dyke Parade, Cork, Ireland

(Received 1 May 2012; accepted 27 August 2012; published online 11 September 2012)

The deposition by atomic vapor deposition of highly *c*-axis-oriented Aurivillius phase $\text{Bi}_5\text{Ti}_3\text{FeO}_{15}$ (BTFO) thin films on (100) Si substrates is reported. Partially crystallized BTFO films with *c*-axis perpendicular to the substrate surface were first deposited at 610 °C (8% excess Bi), and subsequently annealed at 820 °C to get stoichiometric composition. After annealing, the films were highly *c*-axis-oriented, showing only (00*l*) peaks in x-ray diffraction (XRD), up to (0024). Transmission electron microscopy (TEM) confirms the BTFO film has a clear layered structure, and the bismuth oxide layer interleaves the four-block pseudoperovskite layer, indicating the *n* = 4 Aurivillius phase structure. Piezoresponse force microscopy measurements indicate strong in-plane piezoelectric response, consistent with the *c*-axis layered structure, shown by XRD and TEM.

© 2012 American Institute of Physics. [<http://dx.doi.org/10.1063/1.4752007>]

Ferroelectric materials within the bismuth-based Aurivillius family have attracted a great deal of attention from technological, scientific, and environmental points of view.^{1–5} These Aurivillius phases have a series of layered Bi-containing oxides in *c*-axis direction in which $(\text{Bi}_2\text{O}_2)^{2+}$ layers interleave pseudoperovskite blocks, with the formula $(A_{n-1}B_n\text{O}_{3n+1})^{2-}$, where *A* represents monovalent, divalent, or trivalent ions; *B* represents tetravalent, pentavalent, or hexavalent ions; and *n* represents the number of BO_6 octahedra in the pseudoperovskite layer.⁶

The layer-structure compounds within the $\text{Bi}_4\text{Ti}_3\text{O}_{12}$ – BiFeO_3 system combine ferroelectricity with the potential for ferromagnetic properties,⁷ making them attractive for producing films for use in information processing and storage applications. $\text{Bi}_5\text{Ti}_3\text{FeO}_{15}$ (BTFO) is an example of the Aurivillius phase material with of *n* = 4 ($\text{Bi}_4\text{Ti}_3\text{O}_{12}$ – BiFeO_3) and thus has a four-layered perovskite unit of $(\text{Bi}_3\text{Ti}_3\text{FeO}_{13})^{2-}$ sandwiched by two $(\text{Bi}_2\text{O}_2)^{2+}$ layers along *c*-axis.⁸ Previous work undertaken on BTFO has shown it to be both ferroelectric, with a Curie temperature of about 730 °C,⁹ and to possess antiferromagnetic order, with a Néel point of 80 K.¹⁰ The magneto-electric coupling behavior¹¹ and an obvious magnetocapacitance effect¹² have also been observed. By Nd-doping¹³ or by substituting Fe with the Co¹⁴ BTFO, solid-solution films have been reported to exhibit ferromagnetism to some degree, although recent work^{15,16} has shown that great care must be taken, when interpreting ferromagnetic responses, to eliminate the effects of ferromagnetic second phases, even at very low levels. In addition, Jang *et al.*¹⁷ reported the photocatalytic and the photoelectrochemical performance of BTFO material for photo-current generation under visible light ($\lambda \geq 420$ nm).

BTFO material has been investigated in both bulk and thin film forms.^{11–19} While methods such as sol-gel,^{12,19} solid-state reaction,^{17,18} and pulsed laser deposition⁴ have been used to fabricate BTFO films, to date there have been no reports of the use of metalorganic chemical vapor deposi-

tion (MOCVD) methods to deposit $\text{Bi}_4\text{Ti}_3\text{O}_{12}$ – BiFeO_3 system materials, although there have been many reports on the deposition of $\text{Bi}_4\text{Ti}_3\text{O}_{12}$ or BiFeO_3 by MOCVD or liquid-delivery MOCVD.^{20,21} Atomic vapor deposition (AVD) is based on pulsed liquid-injection chemical vapor deposition with a volume of each pulse of the order of microlitres.²² It has been proved that AVD can deposit high-quality high-*k* dielectric or ferroelectric films with a largely uniform film thickness, composition, and electrical properties and is highly suitable for mass production.^{22–24}

A horizontal flow Aixtron AIX 200/FE AVD reactor equipped with pulsed liquid delivery system was used to deposit the BTFO films with $\text{Bi}(\text{thd})_3$ (thd = 2,2,6,6-tetramethyl-3,5-heptanedionate), $\text{Fe}(\text{thd})_3$, and $\text{Ti}(\text{O-iPr})_2(\text{thd})_2$ (O-iPr = iso-propoxide) dissolved in dry toluene as the liquid metalorganic precursors. The concentrations of these precursors are 0.1M and their intrinsic similarity in organometallic chemistry makes them reasonably compatible. The volumetric liquid precursor delivery ratio is set at 5.5:3:1 for $\text{Bi}(\text{thd})_3$, $\text{Ti}(\text{O-iPr})_2(\text{thd})_2$, as well as $\text{Fe}(\text{thd})_3$, where an excess of 10% $\text{Bi}(\text{thd})_3$ is added to compensate the Bi evaporation during post-deposition annealing. The volumes of liquid precursors are measured by liquid flow meters at room temperature.

High purity oxygen was employed as the oxidizing medium with a flow rate of 600 sccm (standard-state cubic centimeter per minute). The reactor pressure and the substrate temperature were fixed to 10 mbars and 610 °C, respectively. Other deposition conditions, such as evaporator temperature (220 °C), injection frequency (1 Hz), and carrier gas flows were varied to find out the optimal deposition conditions. To improve the film uniformity, the substrate susceptor was driven to rotate with a nitrogen flow of 40 sccm. N-type (100) silicon wafer was used as the substrate. Before being loaded into the reactor, the substrate was cleaned with methanol and iso-propanol and dried by nitrogen. To reduce the reaction between the film and Si substrate, oxygen was introduced to reactor at 610 °C, to form a SiO_2 protective layer, before the deposition of BTFO film.

^{a)}Electronic mail: panfeng.zhangtolj@gmail.com.

The crystalline structure of the films was examined by x-ray diffraction (XRD) equipped with a Cu-K α radiation source (PANalytical X'pert PRO). Transmission electron microscopy (TEM) samples were prepared using focused ion beam thinning procedures and examined at 200 kV (JEOL 2100). Energy dispersive (EDX) measurements were obtained on JEOL 2100 instrument equipped with Oxford Instrument EDX detector. Piezoresponse force microscopy (PFM) measurements were conducted on a commercial atomic force microscope (MFP-3DTM, Asylum Research) in contact mode. The surface morphology and the thickness were examined using scanning electron microscopy (SEM).

Figure 1(a) shows the θ -2 θ XRD pattern of the as-grown BTFO thin films on Si. Only three peaks of (008), (0010), and (0014) planes can be observed indicating that the as-grown BTFO is partially crystallized with c -axis perpendicular to the substrate surface. It is reported that the film composition and structure are sensitively affected by the substrate temperature and the precursor delivery ratio.²¹ It is found that at the substrate temperature of 610 °C the film composition is very close to the precursor delivery ratio, which means the liquid precursor supply mixing ratio can be transferred into the as-grown film. In this case, the atomic element ratio in the as-grown film is approximately 5.4:3:1, similar to the liquid precursor supply mixing ratio mentioned above. We speculate that there are two reasons for the accurate ratio transferring: the first is that due to the relative high vaporization temperature all liquid precursors can be vaporized completely and the tube between vaporizer and reactor is maintained at 240 °C without any condensation of gas precursors;²¹ the second is that the substrate surface has similar absorption/desorption efficiency for all gas precursors. The accurate controllability of composition in the deposited film will facilitate the deposition of more complex Bi₄Ti₃O₁₂-BiFeO₃ system thin films with integer or fractional n values.⁷

To get a better crystal structure, the as-grown film was annealed in a conventional furnace at 820 °C for 10 min. (In the fabrication of SrBi₂Ta₂O₉ (SBT) thin film by AVD, the

SBT film was also deposited at low temperature (510 °C) and converted to crystallized film after annealing (750 °C).²⁴) Figure 1(b) shows the θ -2 θ XRD pattern of the annealed BTFO thin film. Up to (0024) plane diffraction peak can be observed and no obvious second or impurity phases are detected, indicating that a well layered Aurivillius phase BTFO film formed. The c -axis lattice parameters, calculated from θ -2 θ peak positions, with weightings according to the intensities of the lines, are 4.14 ± 0.01 nm and 4.104 ± 0.004 nm for the as-grown and annealed films, respectively. The reduction in the c -axis parameter on-annealing indicates a reduction in the out-of-plane stress of ca 1% during the annealing process. As the pre-annealed out-of-plane stress is tensile, the pre-annealed in-plane stress must be compressive. After annealing, the peaks become sharper and the value of FWHM (full width at half maximum) decreases (e.g., the (0014) peak FWHM decreases from 0.56° to 0.29°). A calculation of the average thickness of the scattering particles in the out-of-plane direction using the Scherrer formula applied to all the available peaks, and using the breadth of the Si lines as an in-built peak-breadth standard and again weighting the measurements according to the XRD line intensities, indicated an increase in average grain size from 14.1 ± 1.3 nm to 27.0 ± 4 nm.

Figure 2 shows the surface morphology of the as-grown and annealed BTFO films. For the as-grown BTFO film, the surface is rough and the grains are not well coalesced. The line-shaped grains have lengths between 100 nm and 300 nm. After annealing, most of the grains are coalesced well and possess plate-like morphology forms, which is characteristic of layered structures of Aurivillius phase materials.¹⁹ There is an approximate doubling of the grain size in the in-plane direction, which is in-proportion with the change in grain thickness measured in the out of plane direction reported above. The as-grown film has a thickness of 100 nm and no obvious change is observed after annealing in average thickness.

Figure 3(a) shows the cross-section TEM image of the annealed BTFO/Si sample. The BTFO layer has a clear layered structure and shows a good uniformity within whole thickness. In addition, the film is free of intergrowth of other- n Aurivillius phases.²⁶ An interlayer between the BTFO film and underlying amorphous layer was observed and its thickness is 1–2 nm. Apart from the interlayer, EDX spectra confirm the BTFO film to possess stoichiometric

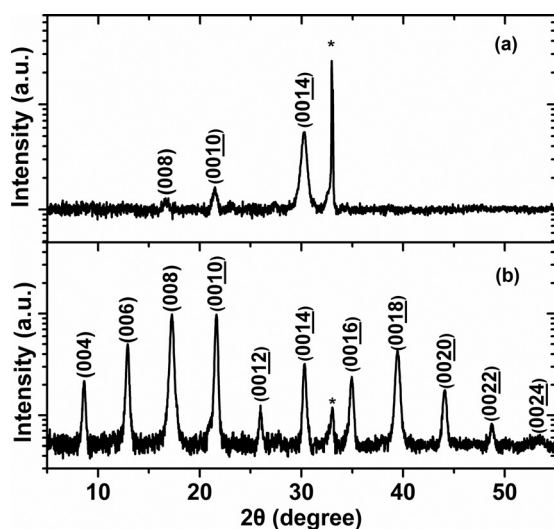


FIG. 1. θ -2 θ x-ray diffraction patterns of the as-grown (a) and annealed (b) Bi₅Ti₃FeO₁₅ films, in which the Si substrate peaks are marked by asterisks.

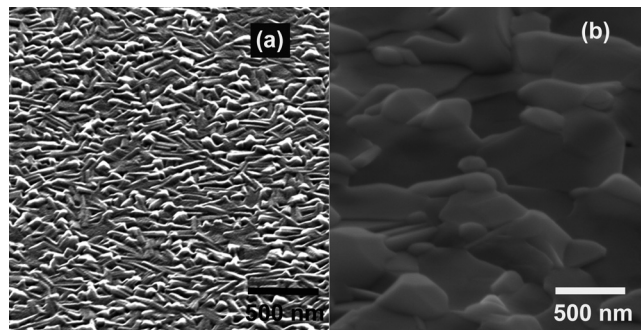


FIG. 2. SEM images of surfaces of the as-grown (a) and annealed (b) Bi₅Ti₃FeO₁₅ films. The images were taken at a tilt of 60°.

composition and the amorphous layer with a composition of SiO_2 . The high resolution TEM (HRTEM) image of annealed BTFO film is shown in Fig. 3(b). The stacking structure of bismuth oxide layer and the four-block pseudo-perovskite layer along c -axis of BTFO can be clearly observed showing the film has the $n=4$ Aurivillius phase. The c -axis lattice parameter measured from HRTEM image is about $4.12 \pm 0.02 \text{ nm}$, in good agreement with that from XRD results.

It is well-known that odd- n -numbered Aurivillius phase materials show minor P_s along the c -axis as well as major P_s along the a -axis while even- n -numbered ones show spontaneous polarization (P_s) only along the a -axis.²⁵ For BTFO with $n=4$ there would be a linear dielectric response on measurements of ferroelectric properties in out of plane direction.^{4,25} So PFM was used to investigate the piezoelectric properties of the films at room temperature. Vertical and lateral single frequency measurements were conducted at a drive frequency of 100 kHz. Vertical PFM images show that there is no obvious phase contrast (Fig. 4(a)) and weak amplitude (Fig. 4(b)). It should be pointed out that the bright areas in Fig. 4(b) are due to the rough grains over surface not the intrinsic piezoresponse, as seen in Fig. 2(b). Lateral PFM images show a strong phase contrast and amplitude contrast as seen in Figs. 4(c) and 4(d), respectively. These results are significantly different from the samples on Si made by sol-gel method, where the orientation of grains is distributed randomly and strong phase and amplitude contrasts are clearly observed in vertical direction.¹⁹

In summary, BTFO thin films were deposited on (001) Si substrates at 610°C by AVD with diluted liquid precursors and the structural and piezoelectric properties were investigated. A SiO_2 layer was formed before the deposition of BTFO layer to reduce the reaction between the BTFO film and Si substrate. The as-grown film was slightly crystallized

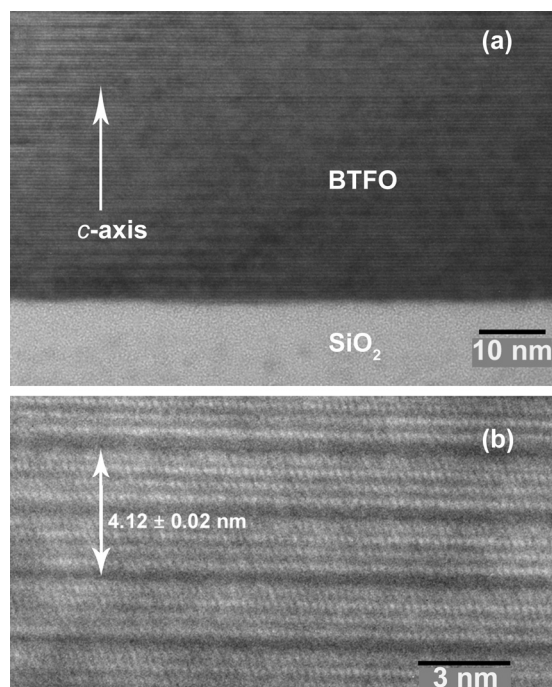


FIG. 3. (a) TEM image taken from a cross section of the annealed $\text{Bi}_5\text{Ti}_3\text{FeO}_{15}$ film. (b) HRTEM image of the lattice structure.

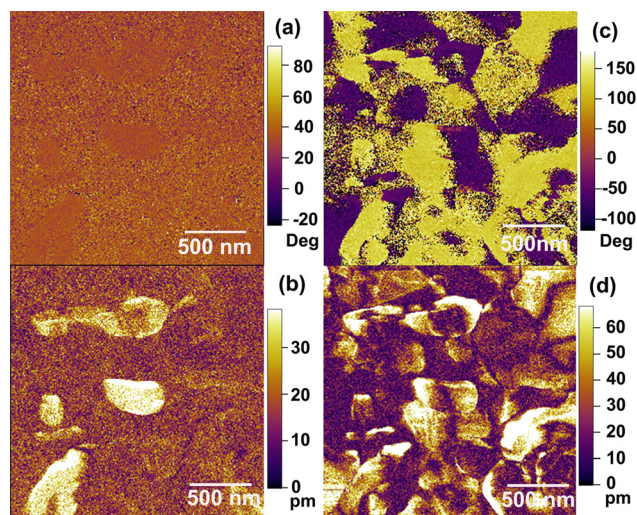


FIG. 4. Piezoresponse force microscope images of the same $\text{Bi}_5\text{Ti}_3\text{FeO}_{15}$ films: (a) vertical piezoresponse phase, (b) vertical piezoresponse amplitude, (c) lateral piezoresponse phase, and (d) lateral piezoresponse amplitude.

with c -axis perpendicular to the substrate surface and post-deposition annealing (820°C , 10 min) was performed to increase the crystallization. In the as-grown film, Bi has an excess of 8% and stoichiometric composition was achieved after annealing. XRD and TEM confirm that the annealed BTFO film has a well-developed c -axis-oriented layered structure with a c -axis length of about $4.104 \pm 0.004 \text{ nm}$. PFM measurements prove that the polar a -axis is parallel with the substrate surface and the BTFO film shows strong in-plane piezoresponse.

The authors acknowledge financial support from Science Foundation Ireland under the FORME Strategic Research Cluster Award number 07/SRC/I1172, the Irish Higher Education Authority (HEA) PRTL13 funding, and HEA PRTL14 Project INSPIRE.

¹B. H. Park, B. S. Kang, S. D. Bu, T. W. Noh, L. Lee, and W. Joe, *Nature (London)* **401**, 682 (1999).

²Y. Noguchi, K. Murata, and M. Miyayama, *Ferroelectrics* **355**, 55 (2007).

³P. K. Panda, *J. Mater. Sci.* **44**, 5049 (2009).

⁴S. Nakashima, H. Fujisawa, S. Ichikawa, J. M. Park, T. Knashima, M. Okuyama, and M. Shimizu, *J. Appl. Phys.* **108**, 074106 (2010).

⁵C.-M. Wang and J.-F. Wang, *Appl. Phys. Lett.* **89**, 202905 (2006).

⁶E. C. Subbarao, *J. Phys. Chem. Solids* **23**, 665 (1962).

⁷N. A. Lomanova, M. I. Morozov, V. L. Ugolkov, and V. V. Gusarov, *Inorg. Mater.* **42**, 189 (2006).

⁸R. E. Newnham, R. W. Wolfe, and J. F. Dorrian, *Mater. Res. Bull.* **6**, 1029 (1971).

⁹A. Snedden, C. H. Hervoches, and P. Lightfoot, *Phys. Rev. B* **67**, 092102 (2003).

¹⁰R. S. Singh, T. Bhimasankaram, G. S. Kumar, and S. V. Suryanarayana, *Solid State Commun.* **91**, 567 (1994).

¹¹A. Srinivas, S. V. Suryanarayana, G. S. Kumar, and M. M. Kumar, *J. Phys.: Condens. Matter* **11**, 3335 (1999).

¹²X. W. Dong, K. F. Wang, J. G. Wan, J. S. Zhu, and J.-M. Liu, *J. Appl. Phys.* **103**, 094101 (2008).

¹³F. Z. Huang, X. M. Lu, C. Chen, W. W. Lin, X. C. Chen, J. T. Zhang, Y. F. Liu, and J. S. Zhu, *Solid State Commun.* **150**, 1646 (2010).

¹⁴X. Y. Mao, W. Wang, X. B. Chen, and Y. L. Lu, *Appl. Phys. Lett.* **95**, 082901 (2009).

¹⁵L. Keeney, S. Kulkarni, N. Deepak, M. Schmidt, N. Petkov, P. F. Zhang, S. Cavill, S. Roy, M. E. Pemble, and R. W. Whatmore, "Room temperature ferroelectric and magnetic investigations and detailed phase analysis of Aurivillius phase $\text{Bi}_5\text{Ti}_3\text{Fe}_{0.7}\text{Mn}_{0.3}\text{O}_{15}$ thin films," *J. Appl. Phys.* (to be published).

- ¹⁶M. Palizdar, T. P. Comyn, M. B. Ward, A. P. Brown, J. P. Harington, S. Kulkarni, L. Keeney, S. Roy, M. E. Pemble, R. Whatmore, C. Quinne, S. H. Kilcoyne, and A. J. Bell, in 2011 International Symposium on Application of Ferroelectrics (ISAF/PFM), Piezoresponse Force Microscopy and Nanoscale Phenomena in Polar Materials, Vancouver, BC, Canada, July 2011.
- ¹⁷J. S. Jang, S. S. Yoon, P. H. Borse, K. T. Lim, T. E. Hong, E. D. Jeong, O.-S. Jung, Y. B. Shim, and H. G. Kim, *J. Ceram. Soc. Jpn.* **117**, 1268 (2009).
- ¹⁸J. Rymarczyk, D. Machura, and J. Ilczuk, *Eur. Phys. J. Spec. Top.* **154**, 187 (2008).
- ¹⁹L. Keeney, P. F. Zhang, C. Groh, M. E. Pemble, and R. W. Whatmore, *J. Appl. Phys.* **108**, 042004 (2010).
- ²⁰J. Schwarzkopf and R. Fornari, *Prog. Cryst. Growth Charact.* **52**, 159 (2006).
- ²¹S. Y. Yang, F. Zavaliche, L. Mohaddes-Ardabili, V. Vaithyanathan, D. G. Schlom, Y. J. Lee, Y. H. Chu, M. P. Cruz, Q. Zhan, T. Zho, and R. Ramesh, *Appl. Phys. Lett.* **87**, 102903 (2005).
- ²²M. Schumacher, P. K. Baumann, and T. Seidel, *Chem. Vap. Deposition.* **12**, 99 (2006).
- ²³P. F. Zhang, R. E. Nagle, N. Deepak, I. M. Povey, Y. Y. Gomeniuk, E. O'Connor, N. Petkov, M. Schmidt, T. P. O'Regan, K. Cherkaoui, M. E. Pemble, P. K. Hurley, and R. W. Whatmore, *Microelectron. Eng.* **88**, 1054 (2011).
- ²⁴P. R. Chalker, R. J. Potter, J. L. Roberts, A. C. Jones, L. M. Smith, and M. Schumacher, *J. Cryst. Growth* **272**, 778 (2004).
- ²⁵H. Funakubo, *J. Ceram. Soc. Jpn.* **116**, 1249 (2008).
- ²⁶K. R. S. Presthi Meher and K. B. R. Varma, *J. Appl. Phys.* **106**, 124103 (2009).